A New Centrebow Design to enhance the performance of High-Speed Catamarans in Rough Seas

Ahmed Swidan[1*], Dane Christophersen[2], and Tristan Bauer[3]

[1]UNSW Canberra at ADFA, Australia. A.Swidan@unsw.edu.au
[2]Royal New Zealand Navy, New Zealand. danec3@utas.edu.au
[3]Austal, Australia. tristan.bauer@utas.edu.au

High-speed catamarans have, over the past three decades, extended their service areas from protected waters to the open ocean where impacts with waves can result in structural damage. The work detailed in this paper investigates the wetdeck slamming loads and corresponding motions experienced by an amended NPL model that is equipped with a generic centrebow when encountering regular waves. The investigation centred on the influence of early flow separation through utilising three interchangeable centrebow configurations and assessing the slam force magnitudes and vertical acceleration. The systematic and random uncertainties associated with the seakeeping test results are quantified in detail. This experimental investigation therefore provides a new dataset for the slam forces on an arched wetdeck structure and motions of catamaran vessels in head seas. It was found that the early water separation when employing two wedge sections would reduce the slam forces by approximately 44% and enhance the vessel's performance when compared with the parent centrebow configuration. The proposed new passive technique presents a step forward towards lighter, faster and comfortable catamarans.

INTRODUCTION

The wave-piercing catamaran (WPC) hull form is capable of high speeds up to 50 knots in open ocean due to the slenderness of each demihull cutting through the water. A catamaran experiences wetdeck slamming when operating in large waves as the wetdeck, the exposed deck area between the two demi hulls of the catamaran, impacts the water surface with a high relative vertical velocity. Wetdeck slamming is a significant design issue for catamarans since it can decrease catamarans' transport efficiency and can cause major structural damage and crew injuries.

During operation within the normal limits of a typical catamaran only the demihulls interact with the water. Operating in sufficiently large sea states, pitch and heave motions may cause the lower most exposed surface of the cross-deck structure connecting the hulls, known as the wetdeck, to impact the water surface. With repeated loading and unloading, fatigue failure becomes increasingly likely, and previous catastrophic failures of catamarans have occurred, despite being design to classification society rules (Swidan, 2016).

Figure 1: Saint John Paul II, Incat catamaran, length overall = 110m (RINA, 2019).

The main area of interest in the design of large wave-piercing catamarans is the impact loading in the vicinity of the centrebow (i.e. the wetdeck and adjacent structures) during immersion (Davidson et al., 2006; Faltinsen, 2006). A centrebow can be described as a partial arched bow form which is truncated at typically 0.2-0.33 LOA and then a flat wetdeck continues aft towards the stern, as shown in Figure 2.

Swidan (2016) proposed a novel winged centrebow geometry to reduce slam loads acting on a 3D bow section of a catamaran hull model impacting with water at approximately constant speeds. Strong relationships between slam force peaks and impact velocity are observed as a function of relative impact angle and centrebow geometry, with a possible reduction for the winged centrebow. Although, the three dimensionality of the water flow in these slam events was characterised. The water impact tests were limited to test catamarans impacting with initially calm water surface in one Degree of Freedom and at a range of relative vertical impact velocities, e.g. 2.5 m/s up to 5 m/s.

Thus, there is a need to continue the previous work conducted by Swidan et al. (2017) and allow a catamaran model with different centrebow configurations to encounter waves, e.g. more realistic scenarios. Since, modifications to the centrebow geometry showed potential reduction in the slamming loads (Swidan, 2016). The purpose of this work is to investigate the effect of employing a catamaran model with three different centrebow configurations to study the influence of an early flow separation on the wetdeck slam severity.

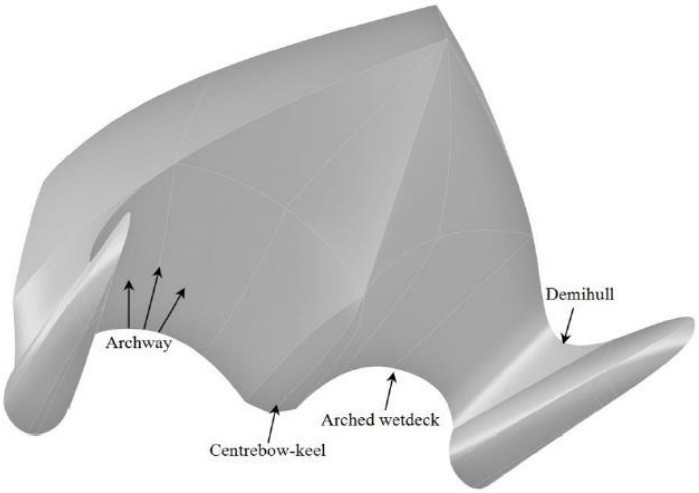

Figure 2: Schematic diagram of bow section for a wave-piercing catamaran. (Swidan, 2016).

MODEL AND EXPERIMENTAL SETUP

The Test System

The model tests were performed in the towing tank facility of the Australian Maritime College (AMC). The AMC's towing tank is 100 m long by 3.55 m wide. Experiments are generally carried out at a water depth of 1.5 m depending on the size and type of model being tested. In this study, a water depth of 1.4 m was necessary to avoid model to carriage possible collisions due to the expected magnitude of model motions. Two disadvantages were recognized utilizing this set-up, 1. the wave-damping mechanism along the side of the tank was ineffective, and 2) the wave maker is calibrated for a water depth of 1.5 m, as such there were slight differences between the target wave heights and the achieved ones during the experimental tests. The hydraulically operated single flap paddle type wave generator produces waves with wavelengths of 0.4-6.5 m and 0.4 m high. A PC based DAQ and processing system is provided to which a variety of analogue and digital instruments can be connected.

The Test Model

The test model was constructed using the National Physics Laboratory (NPL) demihulls and fitted with a generic centrebow, that looks like those used by INCAT, see Figure 4. Figure 4 shows the body plan of the developed catamaran model with the parent centrebow. The model's main particulars are presented in Table 2.

To study the influence of an early flow separation on the wetdeck slam force magnitudes, two interchangeable wedge sections were designed, 3D printed and fitted on the parent centrebow, see Figure 5-I and 5-II. These three model configurations, namely: parent, 35 mm wedge and 45 mm wedge, are shown in Figures 5-I and 6. Figure 6-a shows the width of the horizontal face of the wedges were set to 35 mm and 45 mm, which occupied approximately 20% and 25% of the 180 mm tunnel width at the centrebow truncation, respectively.

Figure 3: Showing the test model attached to the carriage of the towing tank facility at the Australian Maritime College, encountering a wave height of 72.7 mm at a speed of 1.53 m/s.

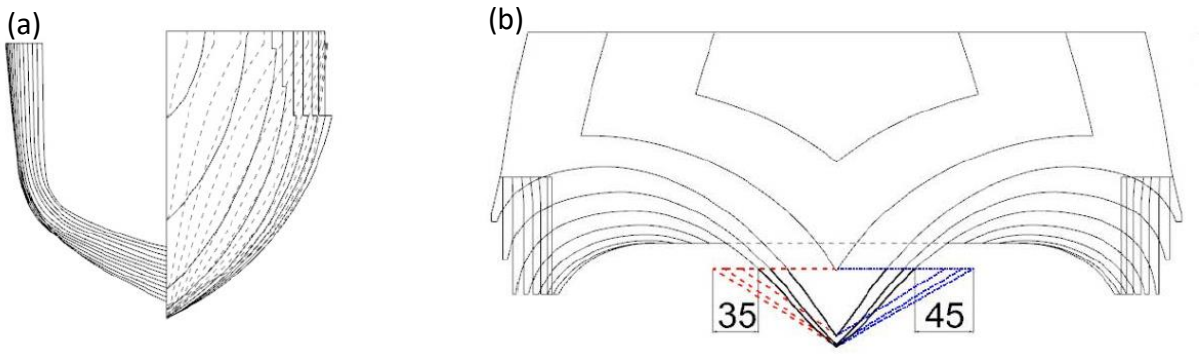

Figure 4: (a) Lines plan for the NPL demihull with amended bow section to fair into centrebow geometry, e.g. the shaded lines are the original demihull sections. (b) Generic centrebow lines for the three interchangeable centrebow configurations, e.g. parent (lines in black), 35 mm wedge (dash lines in red) and 45 mm wedge (dash lines in blue).

Table 1: Main particulars of the test model

Length Overall	2661 mm
Length Waterline	2502 mm
Draft	115 mm
Longitudinal Centre of Gravity	893 mm
Beam Extents	918 mm
Beam Centres	690 mm
Displacement	52.16 kg

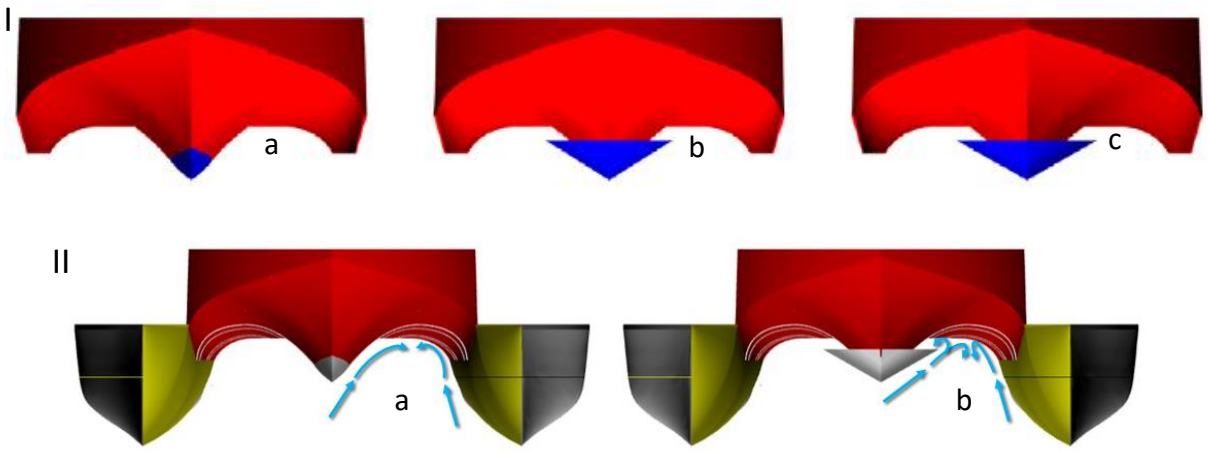

Figure 5: Figure 3 I-a Showing the parent centrebow; (b) 35 mm wedge fitted to parent centrebow; (c) 45 mm wedge. (a), (b) and (c) are viewed from forward and omit the demihulls. Figure 3 II-a showing the semi-entrapped flow behaviour between the parent centrebow and the demihull, (b) illustrates an early flow separation around the tip of the 35 mm wedge.

Instrumentation

To characterise the model's response during impact, the key parameters measured in these tests were: the vertical force, wave profile and the carriage speed. A summary of the instruments and signal conditioning hardware is given in Table 1.

To measure the vertical accelerations, a single MTI inertial sensor was placed on the LCG of the centrebow, as shown in Figure 7. The device consist of a mass-spring system which reside in a vacuum. The sampling rate for recorded data is 400 Hz.

Table 2: Details of Gauges

Gauge	No. of Channels	Manufacturer	Model	Maximum Range
Carriage speed	0	SICK	DME5000	150 m
Load cell	3	Applied Measurement	S1W	350 N
Accelerometer	1	XSENS	MTI-10	5 g
LVDT	3	Hampton	DC-EC-5000	
Static wave probe	2	Static wave probe	SS resistance strips	0.5 m
Moving wave probe	2	General Acoustics	USS 20130	0.5 m

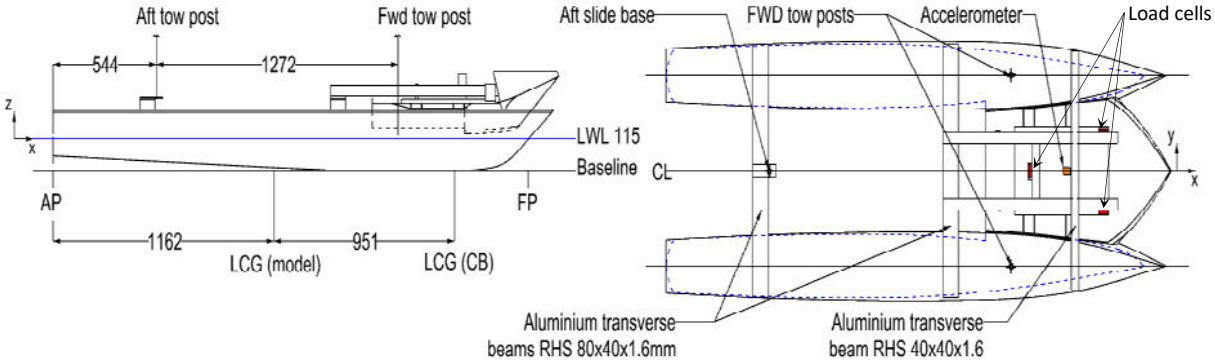

Figure 6: Plan and profile views of the model setup showing locations of load cells and tow posts

Three load cells were considered to be the minimum number sufficient to avoid moments during the impact phase based on recent drop-test experiments, such as those of Swidan et al. (2016). All the total impact force measurements presented in this paper are the sum of the three load cell outputs, as shown in Figure. 7. The model was attached to the carriage by two tow posts, allowed to move freely in the vertical direction within linear slides, to which DC-EC series LVDT sensors were attached to capture pitch and heave data.

Wave heights were recorded primarily by a static wave probe, e.g. SS resistance strips, located 9 m forward of the wave-maker. Supplementary to this were two moving wave sensors to capture the instantaneous wave profile the model was encountering. These were attached to the carriage with one abreast the LCG of the centrebow and the other abreast the LCG of the model.

A video camera recording at 1920 x 1090 resolution at 25 frames per second was set up immediately forward of the vessel as close to the water surface as possible to view the flow within the centrebow tunnels. The signals from all the instruments were acquired using a modular National InstrumentsTM compact data acquisition system (cDAQ 9174) with National Instruments LabVIEW software used to record the signals. A sampling rate of 10 kHz was used.

Test Conditions

The three centrebow configurations were all subject to the same test conditions. Overall, there were 18 conditions in total, with 3 test runs each to ensure repeatability of the recorded data. Prior to the testing starting, 20 runs were performed to assess the model and instrumentation quality. The two speeds of 1.53 m/s and 2.89 m/s, and initial wave frequency of 0.8Hz were common with previous (AlaviMehr, 2016).

The equivalent Froude number of the speeds of 1.53 m/s and 2.89 m/s are of 0.31 and 0.58 respectively, which would represent 20 and 38 knots respectively for a full-scale vessel assuming an approximate scaling factor of 45. Each tested wave height of 75, 90 and 105 mm was non-dimensionalised against the wavelength to give corresponding wave frequencies of 0.876, 0.8 and 0.741Hz, respectively. To present the measured data, the frequencies are shown in non-dimensional circular encounter frequency, w_e^*, which factors in the models heading and speed with respect to the waves. The formula is presented in equation (1).

$$w_e^* = 2\pi f_e \sqrt{\frac{Lwl}{g}} \qquad (1)$$

Table 3: Summary of Test Conditions

Configuration – hull form	Speed [m/s]	Wave height [mm]
Parent hull	1.53	75, 90 and 105
	2.89	75, 90 and 105
35mm Wedge	1.53	75, 90 and 105
	2.89	75, 90 and 105
45mm Wedge	1.53	75, 90 and 105
	2.89	75, 90 and 105

The average water temperature was 18°C, the average air temperature was 20°C and the density of the water was 998.85kg/m^3 for the duration of the testing (ITTC, 2011). The test conditions are summarised in Table 3.

UNCERTAINTY ANALYSIS

To ensure the high quality of the measured data, systematic and random uncertainties were determined. Systematic uncertainties stem from the instrument themselves, and the accuracy of the reading is usually published by the manufacturer. Random uncertainties are caused by factors which are uncontrolled, e.g. environmental.

Systematic Uncertainties

The uncertainties based on the instrumentation used were sourced from the technical data provided by the manufacturers. Table 4 summarises the systematic uncertainties of each instrument used during the experiment. The linearity error is the residual difference between the sensor output curve and line of best fit. Filtering of measured slam forces has been avoided to obtain the peak of the transient slam load magnitudes that occurs within a very short duration of time.

Table 4: Summary of the systematic uncertainty of the instruments

	Carriage position/speed	Load cell	Accelerometer	LVDT	Moving wave sensor
Uncertainty source	Waldkirch DME5000-212	XTran S1W 350N	XSENS MTI-10 series	DC- EC-5000	General Acoustics 20130
Linearity error (%)	0.3	0.03	0.5	0.25	0.18

Random Uncertainties

Each condition, see Table 3, was repeated for a minimum of three runs to confirm that the recorded data was repeatable as well as to provide confidence in the instrumentation being used including the recording DAQ system.

Figures 7 and 8 show good repeatability between the three tests of all measured data using two LVDTs, static wave sensor, carriage speed sensor, accelerometer and three identical load cells. These tests were at 1.53 m/s set carriage speed and 90 mm set wave heights at a set wave frequency of 0.8 Hz.

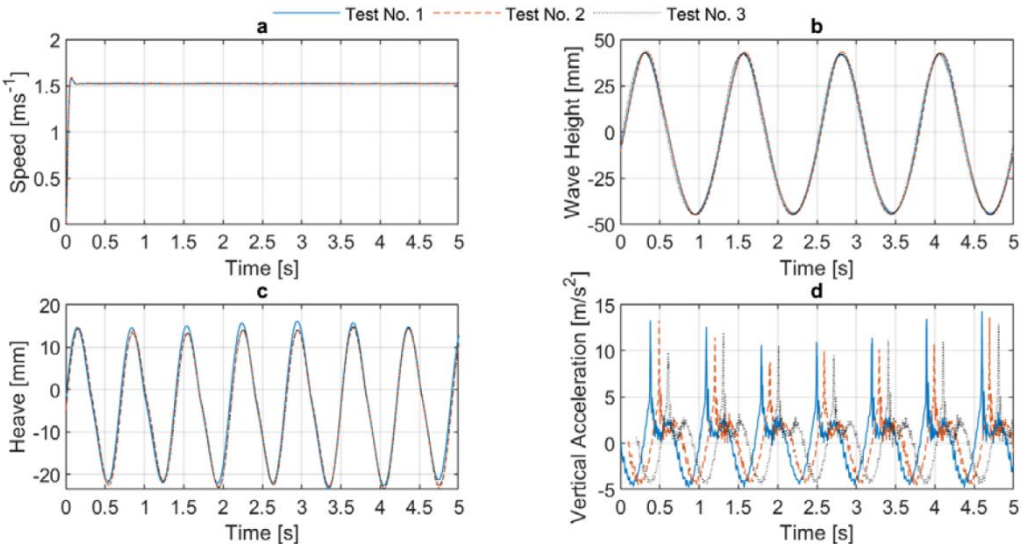

Figure 7: Repeatability of three test runs for the parent configuration in H_w = 84 mm, w_e^* = 4.05 and V_m = 1.53m/s model speed. (a) carriage speed, (b) wave height, (c) heave, (d) vertical acceleration (time axis shifted for better visual comparison).

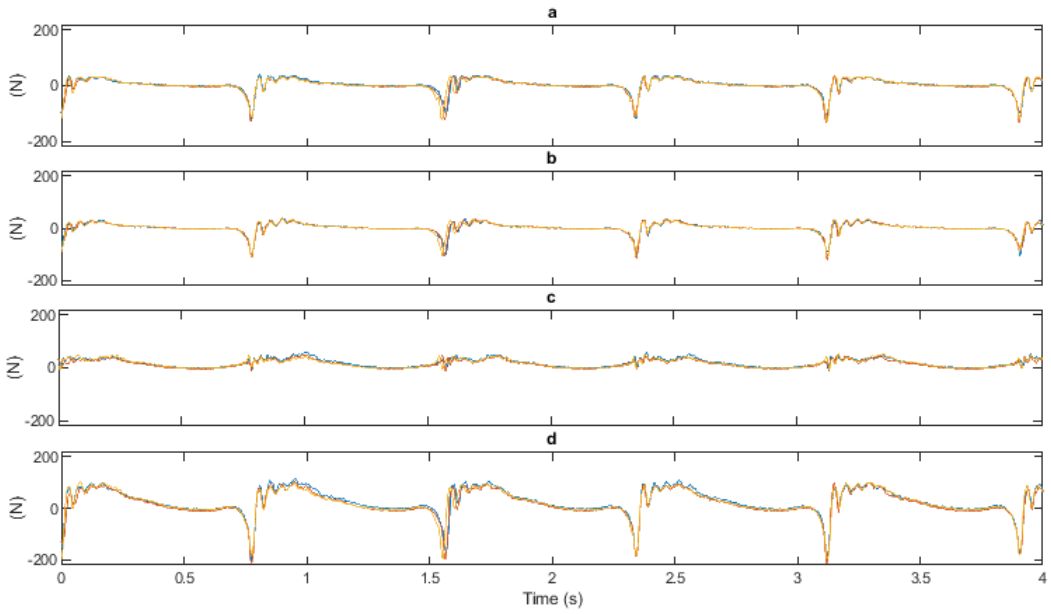

Figure 8: Showing 3 run results of condition 1. The results include (a) the port side load cell, (b) starboard load cell, (c) Aft load cell, and (d) The total load, e.g. instantaneous summation of the three load cell measurements.

Table 5: Summary of recorded wave heights and their respective RMSE and percentage error

Average Wave Height [mm]	RMSE ± [mm]	Error ± [%]
72.74	0.6	1.65
83.71	2.6	6.27
101.19	0.36	0.72

The root mean square error (RMSE) for the peaks of the forward LVDT was 1.43 mm and the aft LVDT RMSE was 1.45 mm over 10 cycles, as shown in Table 5. The steps in the wave data is due to the 50 Hz output of the wave sensor being sampled at 10 kHz as previously described. The static wave probe showed some uncertainty in the wave height produced by the wave generator, as shown in Table 5, with the greatest error found for the wave height of 90 mm at ±6.27%. This was attributed to that the tank was filled at a lower level of water of 1.4 m than what the wave maker was calibrated at, e.g. 1.5 m depth. Some asymmetrical loading was observed with approximately 9.95% greater on the starboard load cell. This was likely due to the asymmetrical mass of the centrebow due to the plugs where pressure sensors have previously been fitted.

RESULTS AND DISCUSSION

The presence of wetdeck slam events, where water impacted the archways, was limited to 9 conditions, which are summarised in Table 6. No wetdeck slam events were recorded in the remaining conditions this deemed to be due to the relatively small wave height with respect to the designed high airgap, which is the vertical distance between the water surface and the top of the arched wetdeck, and/or could be due to the higher wave encounter frequency.

Figure 9 illustrates a corresponding load cycle for both the parent centrebow and the 45 mm wedge configuration in condition '1'. The major characteristics of the trend for the parent centrebow are labelled in Figure 9-a. Figure 9-b shows a small peak in the total load prior to the maximum slam load, which deemed to be when the wedge impacts with the water surface. This minor depression was likely to be significantly reducing the subsequent major slam load. An overlay of the two data sets is shown in Figure 9-c to demonstrate there is a clear difference in the magnitude of the maximum slam load and subsequent vibration, and similar load throughout the remainder of the cycle.

Figure 10 illustrates corresponding images to Figure 9. At time of 0.35 s the wedge forced water transversely outwards during water entry, disrupting the flow of the jet rising up the sides of the demihulls. In contrast the parent centrebow shows relatively smoother water entry. Thus, it is probable that there was a region of trapped air above the horizontal surfaces of the wedges during submersion, as there was visible flow separation occurring during the relative descent of the centrebow.

Table 6: Summary of Test Conditions when Slam Occurred

	Condition	V_m [m/s]	H_W [mm]	h_w	f [Hz]	λ [m]	k	w_e [rad/S]	w_e^*
All hull forms	1	1.53	84	0.12	0.8	2.44	2.5	8.03	4.05
	2	1.53	101	0.11	0.74	2.85	2.2	8.04	4.06
	3	2.89	101	0.11	0.74	2.85	2.2	11.04	5.57

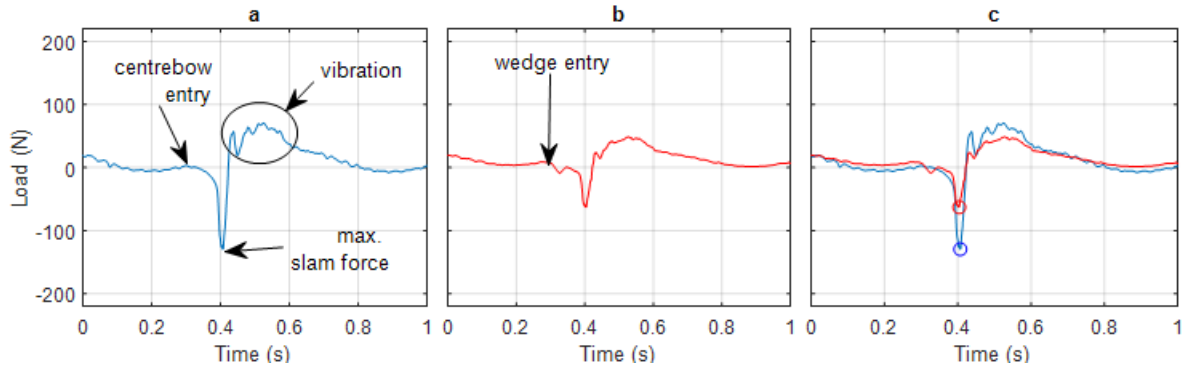

Figure 9: Showing a slam cycle load of (a) parent and (b) 45mm wedge configurations in condition '1', and (c) compares between the two configurations.

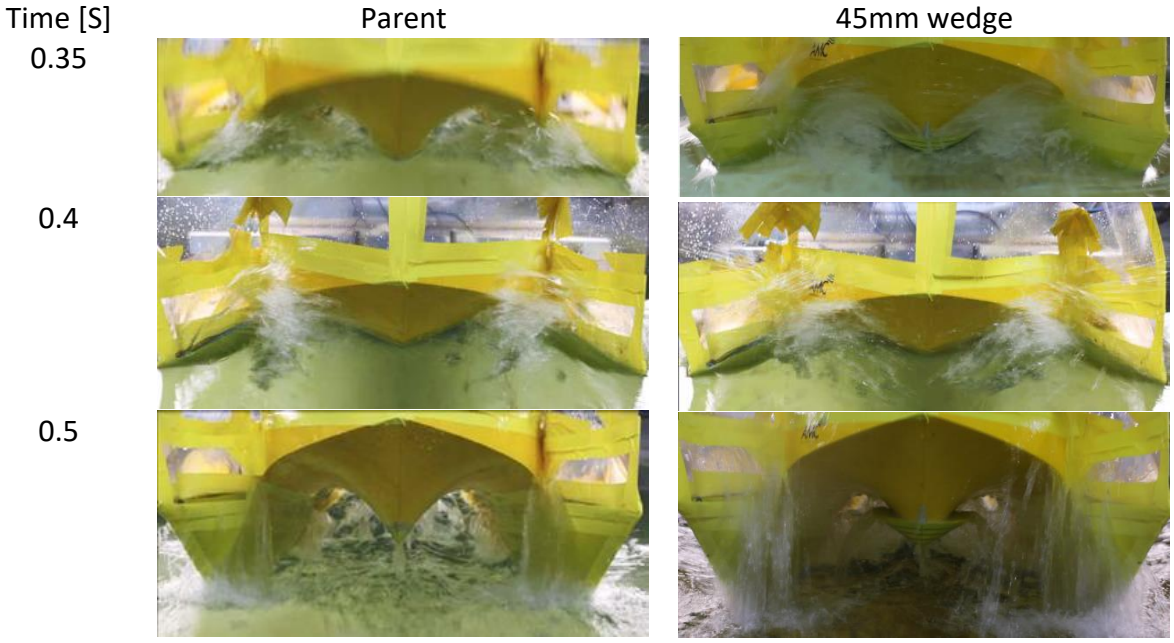

Figure 10: Photos taken of the parent and 45mm wedge configurations during a slam cycle.

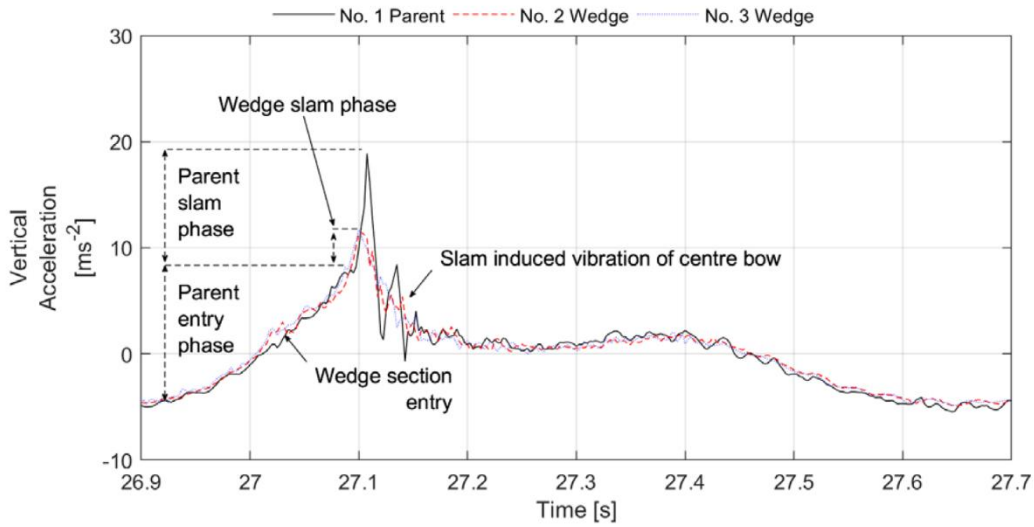

Figure 11: A vertical acceleration signal during a slam event for each centrebow configuration in condition 2. Time axis shifted to align peak accelerations.

Figure 11 analyses a single peak in condition 2. The entry phase for both the parent and wedge centrebows begins when the model is at the maximum possible displacement above the static water line. The acceleration peak of the parent configuration is of 18.9 m/s^2. The 35 mm wedge and 45 mm wedge sections show a 39.5% and 38.1% reduction, respectively. Thus, utilizing the wedges would absorb a greater proportion of the wave energy prior to slam event as well as the wedge upper surface add drag force to the parent centrebow during water exit, as such reduces the model's vertical acceleration.

Figure 13 demonstrates consistency of the previously identified reduction in slam loads across the 10 s sample data for each configuration operating in a condition '1'. Only the points of maximum load are shown to avoid confusion. The plots indicate that the parent centrebow repeatedly experiences the highest slamming loads, while the 45mm wedge offers the greatest reduction. The mean load and percent reduction for each configuration over the 10 s period is shown in Table 8.

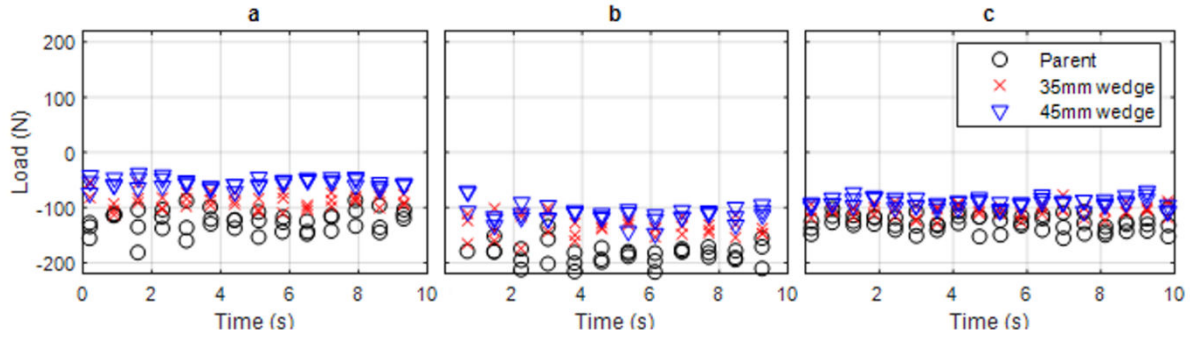

Figure 12: Showing all measured slam peak force magnitudes of conditions 1, 2 and 3.

Table 7: Mean peak load amplitude and percentage comparison per each configuration

		Mean peak force magnitude [N]			Mean peak force [%]		
	Condition	(1)	(2)	(3)	(1)	(2)	(3)
Configuration	Parent	-125	-186	-129	100	100	100
	35mm wedge	-87	-135	-105	69.6	72.6	81.4
	45mm wedge	-55	-112	-90	44	60.2	69.8

CONCLUSIONS

This paper reported on a series of seakeeping tests to investigate the influence of early flow separation on the wetdeck slam force magnitudes by utilizing a generic catamaran hull model that is fitted with three centrebow configurations during wave impacts. In contrast to previous seakeeping tests these experiments focuses on reducing wetdeck slamming loads by allowing the flow to separate prior to slam event rather than modifying using larger or shorter centrebow configurations. Thus, two wedge centrebows were compared against the parent configuration to investigate their effectiveness in reducing the slam force magnitudes and vertical motions of a 2.661m NPL catamaran and generic centrebow model. The parent centrebow used was from an existing design and the wedge sections were interchangeable to create three configurations. Each configuration was tested at two speeds, 1.53m/s and 2.89m/s, and three wave heights, 75mm, 90mm and 105mm.

The systematic and random uncertainties associated with the towing tank test results were quantified in detail and demonstrated a good repeatability of all test results.

Since full details of the generic hull form are presented the results provide a comprehensive set of benchmarking data for use in the validation of numerical techniques to predict slam impact magnitudes of catamarans encountering regular waves.

The largest reduction in total impact loads, observed when utilising the 45 mm wedge to be approximately 44% of the parent centrebow in a condition test condition. The results for the vertical accelerations showed a reduction of 22.1% and 28.0% for the 35- and 45-mm wedge configurations, respectively, when compared with the parent configuration. This was attributed to two main features of the slam event; firstly, water was deflected laterally due to the deadrise of the wedge, and secondly, increasing the truncation volume by 37.6% and 48.1% for the wedge configurations would result in a greater reserve buoyancy than the parent centrebow.

ACKNOWLEDGEMENTS

The Authors would like to acknowledge Dr Jason Lavroff for assistance in the experimental design as well as Mr Tim Lilienthal and Mr Kirk Myer for assistance in the model setup.

REFERENCES

AlaviMehr, J., 2016. The Influence of Ride Control Systems on the Motion and Load Response of a Hydroelastic Segmented Catamaran Model. PhD thesis, University of Tasmania, Hobart, Australia.

Davis, M. R., French, B. J. & Thomas, G. A., 2017. Wave slam on wave piercing catamarans in random head seas. Ocean Engineering, pp. 84-97.

Incat Tasmania (2019). 112m high-speed wave-piercing catamaran. Retrieved 18 Feb, 2019, from: http://www.incat.com.au.

ITTC. (2011). Fresh water and sea water properties. Hjortekaersvej 99: 26th ITTC Specialist Committee on Uncertainty Analysis.

Shabani, B. (2017). *The effects of tunnel height and centre bow length on motions and slam loads in large wave piercing catamarans.* PhD thesis, University of Tasmania, Hobart, Australia.

Shahraki, J. R. (2014). *The Influence of Hull Form on the Slamming Behaviour of Large.* PhD thesis, University of Tasmania, Launceston, Australia.

Swidan, A., Thomas, G., Ranmuthugala, D., Penesis, I., Amin, W., Allen, T. & Battley, M. Experimental drop test investigation into wetdeck slamming loads on a generic catamaran hullform. *Ocean Engineering*, vol. 117C, pp. 143-153. 2016.

Swidan, A. (2016). Wetdeck Slamming Loads– Experimental and Numerical Investigation. PhD thesis, University of Tasmania, Launceston, Australia.

Swidan, A., Thomas, G., Penesis, I., Ranmuthugala, D., Amin, W., Allen, T. & Battley, M. Wetdeck slamming loads on a developed catamaran hullform - Experimental investigation. *Ships and Offshore Structures*, vol. 1, pp.1-9. 2017.